

also support findings from a recent study that adopted a different approach and was conducted at a very different scale, yet also concluded that the prospects for indicator taxa are poor (28). Furthermore, conservation areas identified by means of traditional prioritization criteria [richness hotspots and coldspots and areas containing rare taxa (21)] are unlikely to be useful surrogates for representative complementary conservation networks. This lack of coincidence between taxa, hierarchical levels, and traditional criteria for priority conservation areas implies that all available species-based information should be incorporated into regional conservation assessments (6). Moreover, these results underscore the value of sound species-related distribution data for conservation planning and emphasize the necessity for survey research in conservation biology (29).

REFERENCES AND NOTES

1. P. B. Landres, J. Verner, J. W. Thomas, *Conserv. Biol.* **2**, 316 (1988).
2. R. F. Noss, *ibid.* **4**, 355 (1990).
3. J. Curnutt, J. Lockwood, H.-K. Luh, P. Nott, G. Rüssel, *Nature* **367**, 326 (1994).
4. D. L. Pearson, *Philos. Trans. R. Soc. London Ser. B* **345**, 75 (1994).
5. P. H. Williams and C. J. Humphries, in *Biodiversity*, K. J. Gaston, Ed. (Blackwell, Oxford, 1996), pp. 54–76.
6. K. J. Gaston, *Progr. Phys. Geogr.* **20**, 105 (1996).
7. ———, in (5), pp. 77–113.
8. ——— and P. H. Williams, in (5), pp. 202–229.
9. J. M. Scott *et al.*, *Wildl. Monogr.* **123**, 41 (1993).
10. R. L. Pressey, C. J. Humphries, C. R. Margules, R. I. Vane-Wright, P. H. Williams, *Trends Ecol. Evol.* **8**, 124 (1993).
11. C. R. Margules, I. D. Cresswell, A. O. Nicholls, in *Systematics and Conservation Evaluation*, P. L. Forey, C. J. Humphries, R. I. Vane-Wright, Eds. (Clarendon, Oxford, 1994), pp. 327–350.
12. A. O. Nicholls and C. R. Margules, *Biol. Conserv.* **64**, 165 (1993).
13. D. P. Faith and P. A. Walker, *Biodiv. Conserv.* **5**, 399 (1996).
14. J. R. Prendergast, R. M. Quinn, J. H. Lawton, B. C. Eversham, D. W. Gibbons, *Nature* **365**, 335 (1993).
15. A. T. Lombard, *S. Afr. J. Zool.* **130**, 145 (1995).
16. A. P. Dobson, J. P. Rodriguez, W. M. Roberts, D. S. Wilcove, *Science* **275**, 550 (1997).
17. J. R. Prendergast and B. C. Eversham, *Ecography* **20**, 210 (1997).
18. C. H. Scholtz and E. Holm, *Insects of Southern Africa* (Butterworth, Durban, South Africa, 1995).
19. C. Muller, S. Freitag, C. H. Scholtz, A. S. van Jaarsveld, *Afr. Entomol.* **5**, 261 (1997).
20. K. J. Gaston, *Oikos* **61**, 434 (1991).
21. International Council for Bird Preservation (ICBP), *Putting Biodiversity on the Map: Priority Areas for Global Conservation* (Birdlife International, Cambridge, UK, 1992); World Conservation Union (IUCN), *Centres of Plant Diversity: A Guide and Strategy for Their Conservation* (IUCN, Richmond, VA, 1987).
22. A. G. Rebelo, *Strelitzia* **1**, 231 (1994).
23. K. J. Gaston, *Funct. Ecol.* **6**, 243 (1992).
24. A detailed list providing the degree of overlap between different taxa for complementary sets, richness hotspots, coldspots, and rare taxa is available at www.sciencemag.org/feature/data/975464.shv.
25. J. A. Harrison *et al.*, Eds., *The Atlas of Southern African Birds* (Birdlife South Africa, Johannesburg, 1997); R. M. Cowling and C. Hilton-Taylor, *Strelitzia* **1**, 31 (1994); A. S. van Jaarsveld and S. L. Chown, *S. Afr. J. Sci.* **92**, 459 (1996).
26. C. H. Scholtz and S. L. Chown, *S. Afr. J. Sci.* **91**, 124 (1995).
27. P. H. Williams and K. J. Gaston, *Biol. Conserv.* **67**, 211 (1994).
28. J. H. Lawton *et al.*, *Nature* **391**, 72 (1998).
29. Y. Haila and C. R. Margules, *Ecography* **19**, 323 (1996).
30. Supported by the Foundation for Research Development, the University of Pretoria, the Transvaal Museum, and the Agricultural Research Council. K. J. Gaston and two referees are thanked for comments.

7 October 1997; accepted 2 February 1998

Competition in Retinogeniculate Patterning Driven by Spontaneous Activity

Anna A. Penn,* Patricio A. Riquelme, Marla B. Feller,†
Carla J. Shatz

When contacts are first forming in the developing nervous system, many neurons generate spontaneous activity that has been hypothesized to shape appropriately patterned connections. In *Mustela putorius furo*, monocular intraocular blockade of spontaneous retinal waves of action potentials by cholinergic agents altered the subsequent eye-specific lamination pattern of the lateral geniculate nucleus (LGN). The projection from the active retina was greatly expanded into territory normally belonging to the other eye, and the projection from the inactive retina was substantially reduced. Thus, interocular competition driven by endogenous retinal activity determines the pattern of eye-specific connections from retina to LGN, demonstrating that spontaneous activity can produce highly stereotyped patterns of connections before the onset of visual experience.

The circuitry of the adult nervous system emerges from diffuse sets of early connections (1). Although molecular cues guide initial axonal projections, activity-dependent competition is thought to sculpt precise connections (1–3). Activity-dependent competition driven by visual input from each eye shapes the ocular dominance columns of the visual cortex (3). Likewise, activity-dependent competition between motor neurons shapes connections at the neuromuscular junction (4). Yet precise connections can form in the central nervous system before there is any external sensory input (1, 5). Because many of these connections are highly stereotyped, it is generally thought that they are established in response to molecular cues, rather than by activity-dependent mechanisms (1). However, endogenous neural activity could pattern these connections through a competitive mechanism.

In the mammalian visual system, retinal ganglion cell inputs from each eye, initially intermixed within the lateral geniculate nucleus (LGN), become segregated during development before vision (6–9). Correlated bursts of spontaneous action potentials sweep in “waves” across the retina and are transmitted to the postsynaptic neurons in the LGN during this segregation (10–12). Segregation

of eye-specific layers is dependent on neural activity. When all action potentials in the LGN are blocked by tetrodotoxin (TTX), layers fail to form (13). To directly investigate the role of activity-dependent competition between the inputs from the two eyes in the formation of eye-specific LGN layers, we analyzed the effects of a prolonged and selective blockade of the retinal waves in ferret kits (*Mustela putorius furo*).

Synaptic activation of neuronal nicotinic receptors (nAChR) on ganglion cells is necessary for the generation and propagation of retinal waves (10). Fluorescence imaging experiments (14) were used to monitor large numbers of retinal ganglion cells simultaneously during bath application of cholinergic agents to determine which compounds would block the retinal waves and therefore be potentially useful for *in vivo* intraocular application. Periodic increases in intracellular calcium concentration $[Ca^{2+}]_i$, which are known to be associated with cholinergic synaptic currents measured in ganglion cells (10), are also correlated with bursts of action potentials recorded from ganglion cells (Fig. 1A). Most action potential bursts occurred simultaneously with changes in fluorescence associated with waves propagating through the surrounding tissue [96%; $n = 44$ of 46 bursts recorded in nine cells from five retinas; animals' ages ranged from birth (P0) to postnatal day 9 (P9)].

Both 10 μ M nicotine and 100 μ M curare can block the periodic increases in $[Ca^{2+}]_i$ (10), but these agents are short-acting (10, 15) and thus are poor candidates for intraoc-

Howard Hughes Medical Institute and Department of Molecular and Cell Biology, University of California, Berkeley, CA 94720, USA.

*To whom correspondence should be addressed at 221 Life Sciences Addition, University of California, Berkeley, CA 94720, USA. E-mail: apenn@uclink2.berkeley.edu
†Present address: National Institutes of Health, 36 Convent Drive, MSC-4152, Bethesda, MD 20892, USA.

ular application and maintained blockade. The nAChRs involved are insensitive to 200 nM α -bungarotoxin, which suggests that nAChRs containing the $\alpha 7$ subunit are unlikely to underlie retinal wave propagation (10, 15). Adult rabbit retinal ganglion cells are also insensitive to this drug (16). We tested conotoxins known to affect the other nAChR subunits ($\alpha 3$, $\alpha 4$, $\beta 2$, and $\beta 4$) (17, 18) that are transcribed in the developing rat retina (19). α -Conotoxin MII (1 μ M), which blocks $\alpha 3\beta 2$ expressed in oocytes and synaptosomes (18), produced a complete, reversible block of the waves (Fig. 1B). At lower concentrations (20 nM and 200 nM), α -conotoxin MII decreased the amplitude of the fluorescence changes ($n = 6$) or produced a complete but short-term blockade (<5 min, $n = 3$) (20, 21). α -Conotoxin Au1B (5 μ M), which blocks $\alpha 3\beta 4$ in oocytes (17), did not block waves (Fig. 1B). A recombinant form of κ - (neuronal) bungarotoxin (22), a subtype that causes prolonged, complete blockade of $\alpha 3$ -containing receptors in the presence of nicotine and blocks adult retinal ganglion cell responses to nicotine (15, 16), substantially decreased the amplitude of the fluorescence changes due to the waves (Fig. 1C) or produced a complete blockade followed by partial recovery with drug washout. Thus, cholinergic synaptic transmission via neuronal nAChRs, most likely containing the $\alpha 3\beta 2$ subunits, is required for retinal waves.

Neither α -conotoxin MII nor κ -bungarotoxin is optimal for use in vivo because of rapid reversibility (MII) or partial blockade at lower concentrations (κ -bungarotoxin). On the other hand, (+)-epibatidine, a potent agonist (23) that binds to nAChRs on adult ganglion cells with extremely high affinity (24), blocks the periodic $[Ca^{2+}]_i$ increases at 1 nM concentration (Fig. 1D) through receptor desensitization (25). Even after a 1-hour rinse after 1 nM (+)-epibatidine application, recovery was only partial. No recovery occurred with concentrations ≥ 10 nM ($n = 2$). Application of epibatidine (5 to 10 nM) resulted in a complete blockade of spikes when individual neurons in the ganglion cell layer were recorded, confirming that the blockade of retinal waves, as imaged with calcium-sensitive dyes, corresponds to a blockade of ganglion cell firing (Fig. 1E) (14). The blockade of action potentials was followed either by a washout ($n = 1$) or a demonstration of the neuron's continued ability to spike in response to a depolarizing current injection ($n = 5$). Finally, the nAChR antagonist nereistoxin (NTX), which was previously reported to block nAChRs reversibly in the chick retina (26), blocked retinal waves (Fig. 1F). This blockade, which was due to chemical reduction of the receptor, was reversible by addition of the

nonselective oxidizing agent dithiobis(nitrobenzoic acid) (DTNB) (26). The prolonged blockades provided by these two agents indicate that they are excellent candidates for intraocular injections.

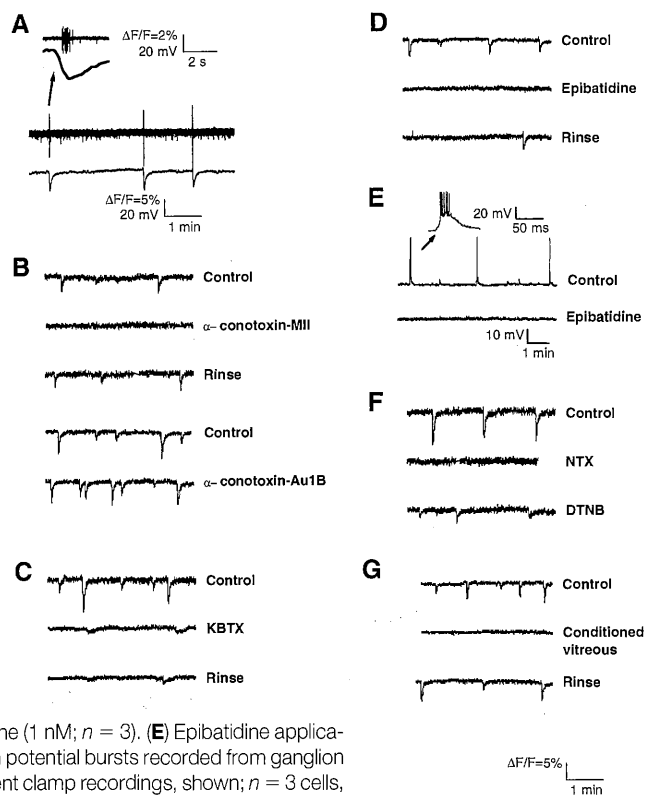
Epibatidine was injected monocularly in ferret kits every 48 hours during the first nine postnatal days (P0 to P9) (27), when retinal ganglion cell axons segregate into eye-specific layers in the LGN (7). Agents were injected along with latex microspheres that had been soaked in the same concentration of drug (28) to provide prolonged release (29). To verify that epibatidine retains its ability to block waves after prolonged in vivo treatment, the vitreous humor from treated retinas was removed and applied to a fresh retina in vitro. Incubating a fura-2AM-loaded retina with the conditioned vitreous humor from neonatal ferrets that received an intraocular injection of epibatidine 48 hours previously or that had a full course of injections every 48 hours from P0 to P9 consistently and reversibly blocked the retinal waves (Fig. 1G). Thus, epibatidine applied with microspheres provides a continuous blockade of retinal ganglion cell activity in vivo.

To examine the consequence of pro-

longed monocular retinal blockade on the segregation of retinal ganglion cell axons within the LGN, at the conclusion of the period of blockade, the axons in the treated and the untreated eye were anterogradely labeled by intraocular injection of two different tracers [either horseradish peroxidase (HRP)-conjugated lectin from *Triticum vulgare* [wheat germ agglutinin (WGA)-HRP] or [3 H]leucine (6, 27)]. The segregation of eye inputs from an initially intermixed state (Fig. 2A, P1) occurred normally between P0 and P9 in animals receiving repeated monocular control injections of saline vehicle (Fig. 2B) (7). The projection from the untreated eye to the contralateral LGN sorted into layers A and C, whereas that from the untreated eye to the ipsilateral LGN sorted into layer A1 (Fig. 2B). [The contralateral projection exclusively occupied a large monocular region of the LGN as well (Fig. 2B, arrowheads).] The projection from the saline-treated eye had a normal complementary pattern (Figs. 2B and 3A).

In contrast, the pattern of ocular inputs after monocular cholinergic blockade was substantially altered (Fig. 2, C through E). After monocular injections of epibatidine be-

Fig. 1. Nicotinic agents block spontaneous retinal waves in vitro. (A) Extracellularly recorded bursts of action potentials (upper trace) are coincident with spontaneous retinal waves simultaneously measured with fura-2AM fluorescence imaging ($\Delta F/F$ averaged over an area of tissue 50 by 50 μ m², lower trace) in the ganglion cell layer. The arrow indicates a burst shown on an expanded time scale (upper trace). (B) Bath application of α -conotoxin MII (1 μ M) reversibly blocks fluorescence changes associated with waves ($n = 3$). α -conotoxin Au1B (5 μ M) does not block the fluorescence changes ($n = 3$). (C) Recombinant κ -bungarotoxin (7 μ M, 45-min incubation) gives partial but prolonged blockade of waves ($n = 3$) or complete blockade ($n = 1$; not shown in figure). (D) Blockade of waves occurs with bath application of epibatidine (1 nM; $n = 3$). (E) Epibatidine application (5 to 10 nM) abolishes action potential bursts recorded from ganglion cells ($n = 5$ cells, whole-cell current clamp recordings, shown; $n = 3$ cells, extracellular recordings). Action potentials could be evoked by current injection during blockade (not shown in figure). (F) NTX (1 μ M, shown, $n = 2$; 100 μ M, $n = 2$) blocks waves and requires channel reoxidation for partial recovery (lower trace in ACSF after a 10-min application of 1 mM DTNB). (G) Vitreous humor from an eye treated with epibatidine injections every 48 hours for 9 days in vivo blocks waves in a fresh retina loaded with fura-2AM (48 hours after injection, $n = 3$; injections made from P0 to P9, $n = 2$). All control traces were made in oxygenated ACSF (14), drugs were applied in oxygenated ACSF, and rinse traces were made after 60 min in ACSF after drug application. Scale bar below (G) applies to (B) through (D), (F), and (G).



tween P0 and P9, the projection from the untreated eye to the contralateral LGN (Fig. 2C) occupied the entire nucleus, with no gap where layer A1 from the other eye should have formed. [The small gap in the projection near the optic tract, present in both saline- and toxin-treated animals, contained a nonretinal projection (30).] The untreated eye's projection to the ipsilateral LGN occupied almost half of the LGN (Fig. 2, C and D, and Fig. 3) rather than refining into layer A1 (which normally occupies about 20% of the LGN at P9). This expansion of territory occurred primarily within the binocular region of the LGN, where competitive interactions between the two eyes would be expected. There was only modest expansion (Fig. 2C, yellow) into the portion of the LGN receiving exclusively monocular input from the other eye (Fig. 2C, arrowheads) (7, 31).

In all cases, the large increase in the projection from the untreated eye after epibatidine injections was complemented by a substantial decrease in the projection from the treated eye (Fig. 2C). The ipsilateral projection from the treated eye was entirely missing (in 5 of 13 cases) or barely detectable (in 8 of 13 cases) (32). The contralateral projection from the treated eye was absent in the normally binocular region of the LGN (in 9 of 13 cases). However, the treated eye's projection was always present in the monocularly innervated segment of the LGN (Fig. 2C, arrowheads). This segment receives axons from the far nasal retina of the contralateral eye only, and no eye-specific layers ever form in this region. Its presence even after blockade indicates that ganglion cells in the treated eye had not merely been damaged or killed, and further demonstrates that retinotopic (as opposed to eye-specific) targeting rules are still being obeyed even though retinal activity has been blocked (1). In some cases (4 of 13 cases), the contralateral projection from the treated eye did not withdraw fully from the LGN's binocular region; instead, the remaining fibers were scattered through this region, overlapping with the active eye's expanded projection (Fig. 2D) (33). The pattern of projections was the same regardless of which eye (treated or untreated) received which tracer (WGA-HRP or [³H]leucine). Similar results were obtained with monocular injections of NTX from P0 to P9 (Fig. 2E). (See www.sciencemag.org/feature/data/975212.shl for results with κ -bungarotoxin.) Quantification of these observations (Fig. 3) (34) underscores the large increase in the size of the untreated eye's projection at the expense of that from the treated eye.

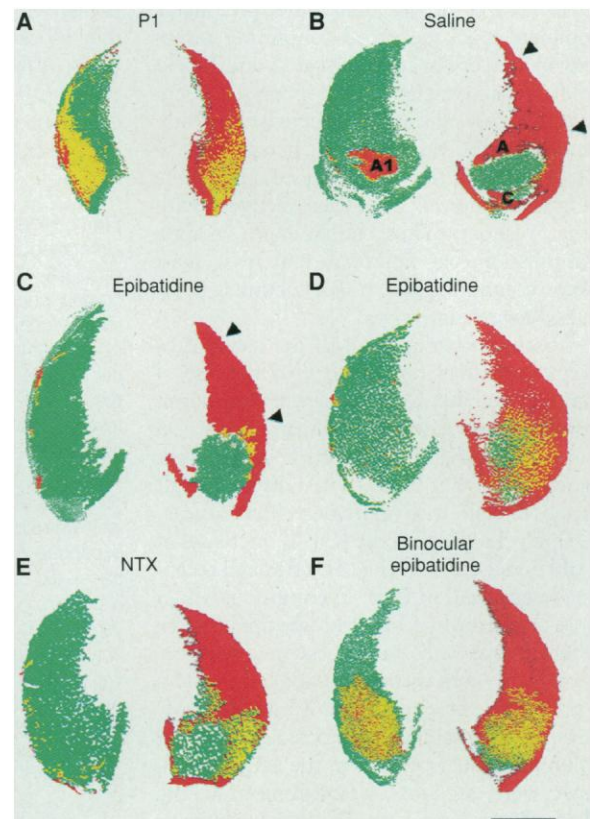
The changes in the eye-specific patterning consequent to monocular blockade with epibatidine or NTX cannot result simply by "freezing" axons from the treated eye in an

earlier immature pattern (compare Fig. 2A and Fig. 2, C through E). At P1, the ipsilateral projection occupies about 40% of the LGN area and the contralateral projection occupies 100% (Fig. 2A). However, after monocular cholinergic blockade, the ipsilateral projection from the treated eye occupies only about 2% of the LGN, whereas that from the untreated eye occupies approximately 50% of the total area. Consequently, axons from the treated eye must actively retract from territories that they had occupied at P1, and the ipsilateral projection from the untreated eye must expand. In contrast, when epibatidine was injected binocularly, the projections from both treated eyes expanded to fill the binocular portion of the LGN (Figs. 2F and 3), which is similar to the effects of intracranial infusion of TTX (13). Our results support a requirement for interocular activity-dependent competition in the

formation of the eye-specific layers, because the projection from the active eye has expanded at the expense of that from the inactive eye after an imposed imbalance in retinal activity, whereas a bilateral blockade of retinal activity results in an equal expansion of both projections.

The altered pattern of the retinogeniculate projection after monocular cholinergic blockade is not due to retinal damage or other nonspecific effects of the drug treatments (Fig. 4). All retinas removed from ferrets after 9 days of intraocular epibatidine injections recovered from blockade and sustained normal waves when imaged (Fig. 4A) (35). In treated retinas, no mechanical damage was observed and overall cell density appeared normal (Fig. 4B) (36). Compound action potentials from the optic tract measured after stimulation of the treated optic nerve were unaffected by epibatidine (Fig.

Fig. 2. Intraocular cholinergic blockade of retinal waves disrupts eye-specific layer formation in the LGN. Retinogeniculate projections from the right eye were labeled by anterograde transport of [³H]leucine (green). Projections from the left eye were labeled by anterograde transport of WGA-HRP (red). Yellow indicates the overlap between the projections. (A) P1 ferret LGN shows initial overlap in projections from the two eyes. (B) Normal pattern of eye-specific layers at P9 in the LGN of animals receiving monocular saline injections between P0 and P9 (*n* = 8 animals treated with saline alone; *n* = 8 animals treated with saline plus microspheres). Projections from the saline-treated eye (red) are segregated into layers A and C on the contralateral side (left) and into layer A1 on the ipsilateral side (right). Projections from the untreated eye (green) have the complementary pattern. Arrowheads denote the monocular region. (C and D) Monocular epibatidine injections after the retinal projection pattern (*n* = 4 animals treated with epibatidine; *n* = 9 animals treated with epibatidine plus microspheres). Projections from the untreated eye (green) fill the entire contralateral LGN (left), and the projection expands considerably in the ipsilateral LGN (right). Projections from the epibatidine-treated eye (red) have withdrawn from the contralateral LGN (right) and are missing entirely from the ipsilateral LGN (left). There is an asymmetry in the effect of epibatidine treatment in that the projection to the monocular region of the LGN contralateral to the treated eye (arrowheads) is maintained, as is expected because there are normally no layers here. (C) The most common projection pattern seen after monocular epibatidine treatment (9 of 13 cases). (D) In 4 of 13 cases (see text), projection from the epibatidine-treated eye to the contralateral LGN did not withdraw completely, causing a larger area of overlap between the two eyes' projections [yellow; compare (C) and (D)] (33). (E) Monocular injections of NTX reveal a similar disruption of LGN layer segregation (*n* = 2 animals). (F) Binocular injections of epibatidine (*n* = 6 animals) cause expansion of projections from both eyes, resulting in extensive overlap (yellow). In all panels, the plane of section is horizontal (at the mid-level of the LGN). Adjacent sections processed for ³H or HRP labeling were superimposed to create a composite pseudocolor image. Medial is toward the midline of each panel; rostral is toward the top of the page. Scale bar = 500 μ m for ³H-labeled sections and 400 μ m for HRP-labeled sections. The methods used are described in (27, 28).



4C; compare upper and lower traces) (37). Moreover, the expansion of axonal territories after binocular injections of epibatidine (Figs. 2F and 3) indicates that the treatment itself does not retard the growth of retinal axons. Another concern is that even though the cholinergic drugs were injected intraocularly, sufficient quantities could have spread beyond the retina to cause a central effect. However, injection of epibatidine plus microspheres directly into the lateral ventricle from P0 to P9 (Fig. 4D) (38) did not alter

eye-specific lamination in the LGN (Figs. 3 and 4D; compare to Fig. 2B). Although changes in receptive field properties and dendritic morphology after cholinergic blockade are seen in turtle retina (39), and retinal activity may be necessary for ganglion cell survival *in vitro* (40), our experimental treatments over the 9-day period used here did not affect the physiological function of the ganglion cells or their axons, nor did they exert their effects directly on nAChRs in the LGN (19, 41).

Fig. 3. Percentage of the LGN occupied by the retinal projections after injections. Solid bars, area occupied by projections from either eye to the contralateral LGN; open bars, area occupied by projections from either eye to the ipsilateral LGN. Results are shown for monocular saline injections ($n = 11$ animals), monocular injections of epibatidine ($n = 10$ animals) or NTX ($n = 2$ animals), binocular injections of epibatidine ($n = 6$ animals), and ventricular injections of epibatidine (38) ($n = 3$ animals; also see Fig. 4D). Statistically significant changes ($P < 0.001$, compared with the corresponding saline-treated projection) are indicated by an asterisk; see also (33). Error bars indicate the standard deviation of the mean. The methods used are described in (34).

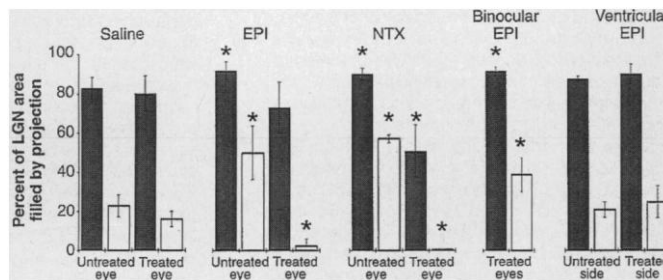
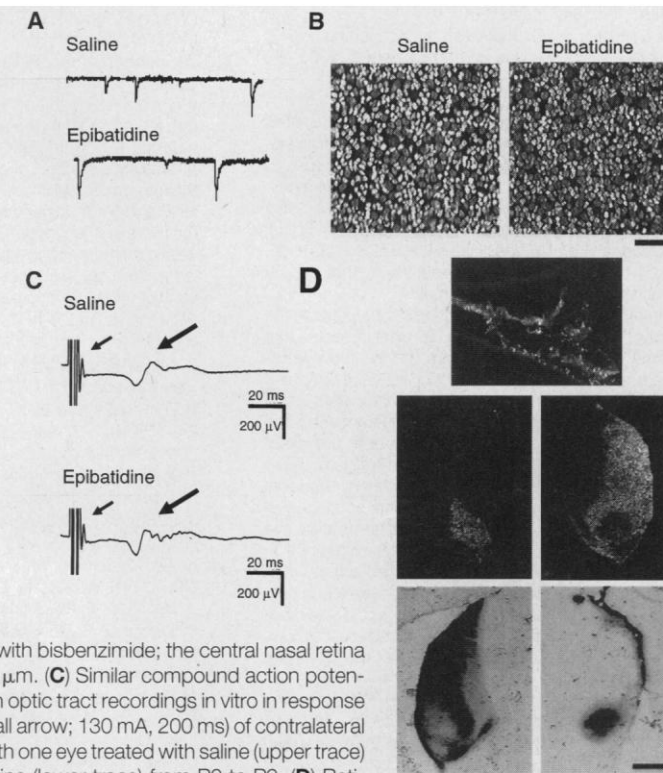


Fig. 4. Eye injections do not damage the retina or act systemically. (A) Washout of drug after 9 days of epibatidine treatment restores retinal waves as assessed *in vitro* by fluorescence changes (35). Top trace, retina treated with saline plus microspheres; bottom trace, other retina from the same animal treated with epibatidine plus microspheres (vitreous humor from this eye blocked retinal waves; see Fig. 1G). (B) Cell densities are unchanged in retinas from ferrets monocularly injected with either saline plus microspheres (left, $n = 3$) or epibatidine plus microspheres (right, $n = 3$). Nuclear staining was done with bisbenzamide; the central nasal retina is shown. Scale bar = 500 μm . (C) Similar compound action potentials (large arrow) are seen in optic tract recordings *in vitro* in response to electrical stimulation (small arrow; 130 mA, 200 ms) of contralateral optic nerves from a ferret with one eye treated with saline (upper trace) and the other with epibatidine (lower trace) from P0 to P9. (D) Retinogeniculate projection is not altered by epibatidine plus microspheres injected directly into the right lateral ventricle from P0 to P9 (38). Single top panel: fluorescent microspheres (labeled with fluorescein isothiocyanate) in the choroid plexus and ventricular space. Bottom four panels: retinal projections from each eye segregate into eye-specific layers. Top pair of panels: left eye injected with [^3H]leucine (silver grains appear white in dark-field optics). Lower pair of panels: right eye injected with WGA-HRP (the transported label is black in bright-field optics). Scale bar = 500 μm for ^3H -labeled sections, 400 μm for HRP-labeled sections, and 100 μm for the ventricle.



By creating an imbalance in activity between the two eyes by monocular blockade, we demonstrated that the balance of active inputs from each eye, rather than overall levels of activity, determines the patterning of retinogeniculate projections from the two eyes. Previous studies in which one eye was removed early in development (42) suggested a requirement for competitive interactions but could not determine whether the competitive mechanism was activity dependent. Conversely, studies in which all activity was blocked by intracranial infusion of TTX (13), or retinogeniculate transmission was disrupted by application of *N*-methyl-D-aspartate receptor antagonists (43), demonstrated a requirement for neural activity in the formation of retinogeniculate connections but could not determine whether competition between the inputs from the two eyes was involved. Likewise, studies in which retinal activity was blocked intraocularly during later periods in the development of the LGN did not address the role of competitive interocular interactions, because segregation at later times occurs between the “on” and “off” ganglion cell axons from a single retina, all of which had been silenced (44). Our experiments define the role of activity and competition. They further demonstrate a direct involvement of the spontaneous retinal waves in this process.

The results of our study extend our understanding of the extent to which neural activity does, and does not, contribute to the final patterning of connections between retina and LGN during development. We observed that the effects of blocking retinal activity in one eye or in both eyes were confined predominantly to the binocular region of the LGN; axons from the ipsilateral eye did not expand substantially into the monocular crescent, even though this region contains only the silenced axons from the contralateral eye (Fig. 2). This observation is consistent with the idea that topographic patterning cues used to set up initial coarse retinotopic maps in the two eyes are likely to be activity independent, as has been reported in other regions of the developing visual system (1, 45). The results also argue against another possibility—that strict eye- or layer-specific molecular cues are present but their expression is activity dependent. If this were the case, in the monocular blockade experiment the active eye’s inputs should have segregated into layers and the inactive eye’s inputs should have expanded, but the pattern seen is just the opposite. Thus, although molecular cues and gradients are likely to be found within the LGN, our experiments emphasize the great extent to which even the earliest patterns of eye-specific connections are shaped by activity-dependent competition driven by spontaneous retinal waves.

REFERENCES AND NOTES

- C. S. Goodman and C. J. Shatz, *Cell* **72** (suppl.), 77 (1993); L. C. Katz and C. J. Shatz, *Science* **274**, 1133 (1996).
- M. Constantine-Paton, H. T. Cline, E. Debski, *Annu. Rev. Neurosci.* **13**, 129 (1990).
- C. J. Shatz, *Neuron* **5**, 745 (1990).
- Y. Dan, L. Y. Lo, M. M. Poo, *Prog. Brain Res.* **105**, 211 (1995); Z. W. Hall and J. R. Sanes, *Cell* **72** (suppl.), 99 (1993); Q. T. Nguyen and J. W. Lichtman, *Curr. Opin. Neurobiol.* **6**, 104 (1996).
- R. Yuste, *Sem. Cell Dev. Biol.* **8**, 1 (1997).
- C. J. Shatz, *J. Neurosci.* **3**, 482 (1983).
- D. C. Linden, R. W. Guillery, J. Cucchiari, *J. Comp. Neurol.* **203**, 189 (1981).
- D. W. Sretavan and C. J. Shatz, *J. Neurosci.* **6**, 234 (1986).
- P. Rakic, *Nature* **261**, 467 (1976).
- M. B. Feller, D. P. Wellis, D. Stellwagen, F. S. Werblin, C. J. Shatz, *Science* **272**, 1182 (1996).
- R. O. Wong, M. Meister, C. J. Shatz, *Neuron* **11**, 923 (1993); M. Meister, R. O. Wong, D. A. Baylor, C. J. Shatz, *Science* **252**, 939 (1991).
- R. Mooney, A. A. Penn, R. Gallego, C. J. Shatz, *Neuron* **17**, 863 (1996).
- C. J. Shatz and M. P. Stryker, *Science* **242**, 87 (1988); D. W. Sretavan, C. J. Shatz, M. P. Stryker, *Nature* **336**, 468 (1988).
- Retinas were isolated and labeled with fura-2AM (Molecular Probes), and images of fractional change in fura-2 fluorescence with 380-nm excitation ($\Delta F/F$) were obtained (10). For simultaneous recording of calcium changes and extracellular spikes (10), the cell membrane was not ruptured in the whole cell configuration. For current clamp recordings, the intracellular solution consisted of 98.3 mM potassium gluconate, 1.7 mM KCl, 0.6 mM EGTA, 5 mM MgCl₂, 40 mM HepesPES, 2 mM Na-adenosine triphosphate, and 0.3 mM Na-guanosine triphosphate. Experiments in which retinas were exposed to the vitreous humor taken from eyes that had received earlier intraocular injections were performed by incubating a fresh fura-2AM-labeled retina in an oxygenated chamber containing the vitreous humor and approximately 2 ml of artificial cerebrospinal fluid (ACSF).
- D. S. McGehee and L. W. Role, *Annu. Rev. Physiol.* **57**, 521 (1995).
- W. H. Baldrige, *J. Neurosci.* **16**, 5060 (1996).
- T. Olivera and M. McIntosh, personal communication.
- G. E. Cartier et al., *J. Biol. Chem.* **271**, 7522 (1996); J. M. Kulak, T. A. Nguyen, B. M. Olivera, J. M. McIntosh, *J. Neurosci.* **17**, 5263 (1997).
- M. Zoli, N. Le Novere, J. A. Hill Jr., J. P. Changeux, *J. Neurosci.* **15**, 1912 (1995).
- A. A. Penn, P. A. Riquelme, M. B. Feller, C. J. Shatz, data not shown.
- At high concentrations (>200 nM) Mill can block other nAChR subtypes when they are expressed in oocytes, namely $\alpha 7$ (which is unlikely to be involved, given the insensitivity to α -bungarotoxin) and to a lesser extent $\alpha 4\beta 2$, $\alpha 3\beta 4$, and $\alpha 2\beta 2$ (18).
- J. J. Flordalisi, P. L. James, Y. Zhang, G. A. Grant, *Toxicol.* **34**, 213 (1996).
- B. Badio and J. W. Daly, *Mol. Pharmacol.* **45**, 563 (1994).
- C. A. Kittila and S. C. Massey, *J. Neurophysiol.* **77**, 675 (1997).
- M. J. Marks, S. F. Robinson, A. C. Collins, *J. Pharmacol. Exp. Ther.* **277**, 1383 (1996).
- Y. Xie, W. V. Lane, R. H. Loring, *ibid.* **264**, 689 (1993); Y. Xie, T. McKay, J. McKay, G. S. Jones Jr., R. H. Loring, *ibid.* **276**, 169 (1996).
- All surgeries on ferret kits were performed according to institutional guidelines and approved protocols. Starting at birth (P0) or P1, intraocular injections were performed every 48 hours under inhaled isoflourane anesthesia. The eyelid was opened aseptically and topical anesthetic (Ophthaine) was applied. A 30-gauge needle (attached to a Hamilton syringe via flexible tubing) was inserted at the temporal edge of the limbus into the posterior chamber of the eye. Eyes at P0 received 1 μ l of drug or control solution at a rate of 0.5 μ l per minute. The dose [see (28)] was increased by 20% with each subsequent injection.
- On P8, 5 μ l of 5% WGA-HRP (Sigma) was injected in one eye and, in most cases, 5 μ l containing 500 mCi [³H]leucine (specific activity: 126 Ci/mmol; Amersham) was injected into the other eye. After each injection, antibiotic ointment (1% chloramphenicol) was applied to prevent leakage from the injection site and the eyelid was sutured shut. The procedure was performed under a dissecting microscope to insure visualization of the needle tip. Animals were assessed for weight gain at P9, and no significant difference was found between drug- and saline-treated animals. Twenty to 22 hours after the final intraocular injection, brains were prepared for histology according to procedures in (6). For WGA-HRP histochemistry, a modified tetramethylbenzidine reaction was used. Sections were rinsed in 0.1 M Tris buffer (pH 7.6), reacted in TrueBlue (Kierkegaard & Perry Laboratories, Gaithersburg, MD) for 1 hour, rinsed in H₂O followed by 30% ethanol, soaked in 9% sodium nitroprusside in 30% ethanol for 1 hour, rinsed in 30% ethanol followed by H₂O, and mounted on slides. In animals that also received radioactive tracer, adjacent sections were processed for autoradiography according to procedures in (6).
- Solutions of 1 mM (+)epibatidine-L-tartrate (RBI, Natick, MA) or 100 mM NTX (Waco Chemicals, Japan) were made in sterile physiologic (0.9%) saline. Sterile saline was injected as the control. Solutions containing latex microspheres were made as follows (29): 20 μ l of ion-exchanged fluorescent microspheres (Lumafuor, Naples, FL) (used in most of our anatomy experiments) or nonfluorescent microspheres (CLB-9, Sigma) (used in some of our anatomy experiments and in all in vitro retinal imaging experiments) were added to 50 μ l of drug or control solution, incubated at 4°C overnight, pelleted by ultracentrifugation, and resuspended in 10 μ l of fresh solution for injection.
- D. R. Riddle, L. D. C. Lo, L. C. Katz, *Nature* **378**, 189 (1995); A. Ghosh, A. Antonini, S. K. McConnell, C. J. Shatz, *ibid.* **347**, 179 (1990).
- B. E. Stein, J. G. McHaffie, J. K. Harting, M. F. Huerta, T. Hashikawa, *J. Comp. Neurol.* **239**, 402 (1985).
- G. Jeffery, *Exp. Brain Res.* **82**, 408 (1990).
- The ipsilaterally projecting axons from the treated eye are unlikely to have been killed by the drug because, when treated with binocular epibatidine injections, axons from the treated eye grow exuberantly. Because many ganglion cell axons at this age also have sustaining collaterals to the superior colliculus [A. Ramoa et al., *Proc. Natl. Acad. Sci. U.S.A.* **86**, 2061 (1989)], we consider it more likely that the axons withdrew into the optic tract.
- Visual inspection of the projection contralateral to the epibatidine-treated eye in Fig. 2D (red) indicates that some contralateral axons from the treated eye remain within the binocular zone, rather than being entirely excluded by the projection from the active eye. This may result from slight differences in the time of onset of effective blockade or in the exact age, in hours postpartum, of the animal (it is possible that activity blockade more rapidly influences axonal extension than axonal retraction). This scattering of remaining axons from the epibatidine-treated eye accounts for the lack of quantitative difference in area occupied by the contralateral projection when compared to that occupied by the contralateral projection from the saline-injected eye (Fig. 3) (34), because the threshold used for measurements was chosen to give a maximal estimate of the area filled by the projection [see also (34)].
- LGN sections containing HRP or [³H]leucine-labeled retinogeniculate projections were examined under light- or dark-field illumination, respectively, and the distribution of label was recorded digitally with a charge-coupled-device camera mounted on a Nikon SMU-Z microscope attached to a Macintosh computer running NIH Image. The mid-section of each LGN (where, in normal animals, the eye-specific layers are most distinct) was selected for quantitation. The scanned gray-scale images were filtered to reduce noise; threshold images were made (for brightfield images, 30% above background; for darkfield images, 70%) and the labeled areas were calculated and compared to the total LGN area in that section. Statistical significance was calculated with a Student's *t* test (of two populations).
- Epibatidine-treated retinas sustained waves either after incubation in fura-2AM ($n = 9$ retinas 18 to 48 hours after injection) or after additional washout in ACSF ($n = 1$ retina 48 hours after a single injection; $n = 2$ retinas after a full series of injections from P0 to P9). Recovery of the retinal waves after fura-2AM loading of the retina was expected if the retina was healthy, because the vitreous humor (containing the epibatidine-treated beads) had been removed for imaging and the fura-2AM incubation volume was relatively large (2 ml).
- In several experiments ($n = 3$ epibatidine-treated retinas; $n = 3$ saline-treated retinas), the eyes that received intraocular injections were removed after perfusion and stored in 4% paraformaldehyde in 0.1 M sodium phosphate buffer (PFA in PBS). The eyes were opened, the lens and vitreous humor were removed, tension-relieving slits were made, and the retina was flattened between two glass slides and placed in PFA. The retina was examined under a stereomicroscope for any visible damage and was stained with 0.01% bisbenzamide (Hoechst) in 0.1 M PBS to reveal the overall density of cells in the ganglion cell layer.
- Immediately after the removal of the eyes for imaging, the brain was removed from the skull with the optic nerves attached ($n = 2$ brains; in each animal, one eye was epibatidine-treated and the other eye was saline-treated). The brain was placed in oxygenated chilled ACSF (12) and sectioned coronally on a vibratome to expose the optic tract. The preparation was perfused with oxygenated ACSF in a recording chamber. A glass electrode filled with ACSF was placed in the optic tract, and the nerves were stimulated with suction electrodes. Recordings were obtained with an extracellular amplifier (Walsh Electronics, Pasadena, CA) and digitized (Axon Instruments).
- We performed ventricular injections ($n = 3$ of epibatidine; $n = 3$ of saline) by making a small incision in the scalp and inserting a 30-gauge needle 1.5 to 2 mm lateral and 1 mm dorsal to the bregma suture to a depth of 1.5 mm. The volume and concentrations of solutions injected, the number of injections, and the intraocular injections of neuronal tracers (WGA-HRP and [³H]leucine) were the same as those used for the eye injections. The location of the injection was confirmed by the presence of the fluorescent latex microspheres located throughout the lateral ventricle (Fig. 4D, top panel).
- E. Sernagor and N. M. Grzywacz, *Curr. Biol.* **6**, 1503 (1996).
- A. Meyer-Franke, M. R. Kaplan, F. W. Pfrieger, B. A. Barres, *Neuron* **15**, 805 (1995).
- G. T. Prusky and M. S. Cynader, *Vis. Neurosci.* **1**, 245 (1988).
- D. W. Sretavan and C. J. Shatz, *J. Neurosci.* **6**, 990 (1986); P. E. Garraghty, C. J. Shatz, M. Sur, *Vis. Neurosci.* **1**, 93 (1988).
- J. O. Hohm, R. B. Langdon, M. Sur, *Nature* **351**, 568 (1991).
- K. S. Cramer and M. Sur, *Dev. Brain Res.* **98**, 287 (1997); M. W. Dubin, L. A. Stark, S. M. Archer, *J. Neurosci.* **6**, 1021 (1986).
- U. Drescher, F. Bonhoeffer, B. K. Muller, *Curr. Opin. Neurobiol.* **7**, 75 (1997).
- We thank G. Grant (Washington University, St. Louis) for providing recombinant α -bungarotoxin, B. Olivera and J. M. McIntosh (University of Utah, Salt Lake City) for conotoxins, R. Loring (Northeastern University, Boston) for nereistoxin, R. Coriveau for advice on acetylcholine receptors, and H. Aaron and C. Cowdry for technical assistance. Supported by NIH grant MH 98108 to C.J.S., NIH MSTP Training Grant to A.A.P., and U. C. Berkeley Miller Fellowship to M.B.F. A.A.P. was in the Neurosciences Program at Stanford University. C.J.S. is an investigator of the Howard Hughes Medical Institute.

25 September 1997; accepted 8 January 1998